

Structural Analysis of Microparticles by Confocal Laser Scanning Microscopy

Submitted: January 20, 2000; Accepted June 20, 2000

Alf Lamprecht*, Ulrich Schäfer, and Claus-Michael Lehr

Department of Biopharmaceutics and Pharmaceutical Technology,
Saarland University, Im Stadtwald, D-66123 Saarbrücken, Germany

ABSTRACT This study demonstrates the potential of confocal laser scanning microscopy (CLSM) as a characterization tool for different types of microparticles. Microparticles were prepared by various methods including complex coacervation, spray drying, double emulsion solvent evaporation technique, and ionotropic gelation. Protein drugs and particle wall polymers were covalently labeled with a fluorescent marker prior to particle preparation, while low molecular weight drugs were labeled by mixing with a fluorescent marker of similar solubility properties. As was demonstrated in several examples, CLSM allowed visualization of the polymeric particle wall composition and detection of heterogeneous polymer distribution or changes in polymer matrix composition under the influence of the drug. Furthermore, CLSM provides a method for three-dimensional reconstruction and image analysis of the microparticles by imaging several coplanar sections throughout the object. In conclusion, CLSM allows the inspection of internal particle structures without prior sample destruction. It can be used to localize the encapsulated compounds and to detect special structural details of the particle wall composition.

KEYWORDS: Confocal laser scanning microscopy (CLSM); Microencapsulation; Microparticles; Polymer distribution

INTRODUCTION

Microparticles are common drug delivery systems. Different preparation methods have been applied to optimize their use. The characterization methods are numerous as well. The most widely used procedures to visualize microparticles are conventional light microscopy (LM) and scanning electron microscopy (SEM) [1-5]. Both techniques can be used to determine the shape and outer structure of the microparticles; nevertheless, they both have certain limitations when used for the analysis of the internal structure of such particles.

LM is impeded by the scattering or emission of light from structures outside the optical focal plane, which reduces image quality. On the other hand, SEM usually requires a relatively intensive sample pretreatment and does not permit the visualization of internal structures of objects at all. Mechanical sections of embedded particles allow inspection of the particle wall structure, but the encapsulated phase often gets lost during sample preparation. Furthermore, these techniques do not provide enough information about the particle polymer composition. For many reasons, however, it would be of interest to identify and localize the encapsulated drug or the deposition and distribution of the involved polymers.

Confocal laser scanning microscopy (CLSM) minimizes scattered light from out-of-focus structures, and permits the identification of several compounds through use of different fluorescence labels. Therefore, CLSM can be applied as a nondestructive visualization technique for microparticles. Moreover, CLSM allows visualization and characterization of structures not only on the surface, but also inside the particles, provided the material

***)Corresponding Author:** Alf Lamprecht, PhD
Department of Biopharmaceutics and
Pharmaceutical Technology Saarland University, Im
Stadtwald, D-66123 Saarbrücken, Germany;
e-mail:alla0004@stud.uni-sb.de

is sufficiently transparent and can be fluorescently labeled. By collecting several coplanar cross sections, a three-dimensional reconstruction of the inspected objects is possible.

CLSM has already been used in the evaluation and characterization of solid pharmaceutical formulations, including determination of the release kinetics of the entrapped drugs [6, 7] and examination of the swelling of microparticles by using fluorescein-containing aqueous media [8, 9]. Furthermore, microparticles were visualized in order to depict the dispersion of the entrapped phase [10] and polymer structures on the surface [11] as well as first results in imaging the polymer composition [12].

This study evaluates CLSM as a tool for the characterization of microparticles, especially their internal structure. Experiments were designed to show the applicability of this technique to particles made by different preparation methods and to demonstrate the simplicity and speed of this procedure as well as the value of the additional information that could be gained.

MATERIALS AND METHODS

Materials

Gelatin, types A and B, was purchased from Deutsche Gelatine Fabrik Stoess & Co. (Eberbach, Germany) and acacia was obtained from Caesar & Loretz (Hilden, Germany). Chitosan glutamate was obtained from Pronova Biopolymers (Drammen, Norway) and eicosapentaenoic acid ethyl ester (EPA-EE) with a purity greater than 96% was obtained from K. D. Pharma (Bexbach, Germany). Poly- ϵ -caprolactone, casein, fluorescein isothiocyanate (FITC), and rhodamine B isothiocyanate (RBITC) were purchased from Fluka (Deisenhofen, Germany); polyvinyl alcohol (Moviol 40–88), sodium alginate, calcium chloride, bovine serum albumin (BSA), Nile red, dimethyl sulfoxide (DMSO), and ethanolamine were purchased from Sigma (Deisenhofen, Germany). Ethanol, hydrochloric acid, and methylene chloride were obtained from Merck AG (Darmstadt, Germany). All compounds were of analytical grade purity.

Methods

Preparation of the Microparticles Complex Coacervation

Gelatin, 2.5 g, was dissolved in 100 mL water at 50°C. Then, 5.0 g of oil phase (EPA-EE) was emulsified in the gelatin solution by using an Ultraturrax (8000 rpm, Model T 25, Janke & Kunkel, IKA-Labortechnik, Staufen, Germany). The emulsion was poured into a beaker containing an aqueous solution of acacia (2.5%, wt/vol). Water, 400 mL, was added; the pH was lowered with 1N HCl to 4.0; and the system was cooled to 4°C. After the sedimentation of the microparticles, the supernatant was decanted and the particles were hardened by adding 2 x 150 mL ethanol to the sediment. Finally, the microcapsules were filtered and dried overnight at room temperature.

Spray Drying

The coacervate was prepared as described earlier, with the supernatant removed after sedimentation, and the sediment further processed by spray drying. For the spray-drying process a Büchi 190 Mini Spray Dryer (Flawil, Switzerland) was used; apparatus parameters were chosen after optimization (aspiration: 20; pressure: 300 Nl/h; temperature at inlet: 140°C, at outlet: 80°C).

Double Emulsion Technique

The preparation of microparticles was based on water-in-oil-in-water emulsification-solvent evaporation methods [13, 14]. It was prior optimized as follows: 1 mL of a BSA-FITC containing aqueous solution (10 mg/mL) was first emulsified for 1 minute by Ultraturrax into the polymer solution (800 mg of PCL) in methylene chloride (10 mL). This primary emulsion (w/o) was poured into 300 mL of PVA solution (0.25% wt/wt). A w/o/w-emulsion was formed by extensive stirring with a four-blade stirrer for 45 minutes at 1000 revolutions per minute (rpm). After decanting the supernatant, the microparticles were filtered (HVLP filter, pore size 0.45 micrometers, Millipore, Eschborn, Germany), washed 3 times with water (minimal volume 500 mL) and dried overnight at room temperature.

Ionotropic Gelation

A 1 mL amount of BSA-FITC solution (10 mg/mL) was added to a sodium alginate solution (2% wt/wt). This alginate solution was added in drops to a calcium chloride solution (2% wt/wt) using a syringe with a 0.30-mm needle. In subsequent experiments, 1 mL hydrochloric acid (1N) and chitosan glutamate (final concentration: 0.1% wt/wt) were dissolved in the CaCl₂ solution. When gelation occurred, particles were collected by filtration, washed extensively with water, and dried overnight at room temperature.

Fluorescence Labeling of the Organic Phase by Nile Red

Before preparing the oil-water emulsion, Nile Red was dissolved in the organic phase (EPA-EE for complex coacervation, or methylene chloride for double emulsion technique). As Nile Red has a strong susceptibility to fluorescence bleaching, a concentration of at least 1 mg/mL was used.

Fluorescence Labeling of Gelatin, Casein, Acacia, and Alginate

Based on a method of protein labeling by Schreiber et al. [15], the covalent labeling protocol was adapted to our requirements. Briefly, aqueous protein or polymer solution was adjusted at pH 8.5-11 by sodium hydroxide solution (1N). The resulting fluorescent dye, FITC or RBITC, was dissolved in DMSO at a concentration of 1 mg/mL. A 100 μ L amount of the dye solution was added to the polymer solution and stirred for 1 hour at 40°C. The reaction was stopped by adding 20 μ L ethanolamine; free FITC or RBITC was removed by dialysis (dialysis tube with a 10,000 Dalton pore size) against distilled water until no diffusion of the free marker was observed.

Confocal Laser Scanning Microscopy

A Biorad MRC 1024 Laser Scanning Confocal Imaging System (Hemel Hempstead, UK), equipped with an argon ion laser (American Laser Corp, Salt Lake City, UT) and a Zeiss Axiovert 100 microscope (Carl Zeiss, Oberkochen, Germany), was used to

investigate the structure and morphology of the microparticles. All confocal fluorescence pictures were taken with a 2.5 \times , 10 \times or 40 \times objective (40 \times objective: oil immersion, numeric aperture 1.30). The software used for the CLSM imaging was LaserSharp MRC-1024 Version 3.2 (Bio-Rad, Deisenhofen, Germany). The imaging was performed with dry microparticles or particle dispersions in neutral oil to prevent their swelling during sample imaging.

The laser was adjusted in the green/red fluorescence mode, which yielded two excitation wavelengths at 488 and 514 nm. Emission filter blocks VHS/A1 and A2 were used. Green and red fluorescence images were obtained from two separate channels, with the option of a third picture from the transmitted light detector. The final pictures were composed from mixer A (red fluorescence) and mixer B (green fluorescence) to visualize the marked structures and also the signal from the ordinary transmission light microscope (mixer C - transmitted light) within the same image.

RESULTS AND DISCUSSION

CLSM permits the user to depict and unambiguously identify all fluorescently labeled compounds at light microscopical resolution. Unlike conventional light microscopy, CLSM enables the user to qualitatively determine localization as well as amount of the inner oil phase without having to first establish complex analytical procedures. The identification of the encapsulated phase can also be performed with a non-confocal fluorescence microscope, if the drug is fluorescently labeled. The unique advantage of CLSM is its capability to obtain information about the three-dimensional localization of fluorescently labeled compounds along (x,y,z) spatial dimensions.

It must be kept in mind that nonfluorescent material cannot be detected by CLSM without prior fluorescence labeling. If drug or polymer have solubility properties similar to the fluorescence marker, mixing these may be sufficient, as long as the encapsulation process and the incorporation of the drug will not be altered by the marker. This is the favored method when covalent labeling of macromolecules is inefficient, such as with polyesters (PCL). In case of different solubilities of

marker and drug, covalent coupling is necessary to ensure that the fluorescence marker represents the desired material. Any covalent coupling of marker and drug or polymer must be attempted with caution, as the physico-chemical properties may be considerably changed (especially in the case of low molecular weight drugs).

FITC and RBITC were chosen to allow simultaneous detection in different channels. The concentrations of the fluorescent markers were adjusted according to their stability in the laser light (photobleaching). In some cases, there was a possibility that functional groups could be blocked after the fluorescence labeling step (eg, gelatin and chitosan), and thereafter the polymers could change their properties. However, isoelectric focusing proved no significant change of the isoelectric point for gelatin (ratio of marker molecules to free amino groups, 1:46). For chitosan the amount of added fluorescence marker was much lower than the number of potential binding sites. The negatively charged carboxyl groups of acacia and alginate presented no target for the labeling reaction, and therefore it was reasonable to assume that their properties were not significantly affected by this procedure. After taking into account the labeling efficiency (8% to 19% of the marker was covalently bound), the ratio of molecule fluorescence marker to molecule polymer was rather low (RBITC:acacia = 1:0.36; RBITC:chitosan = 1:0.72); no effects should be expected as the molecular weight of the polymers is about 1000 times larger.

Characterization of Microparticle Structure

Deposition Behavior During Complex Coacervation

Staining the oil phase with Nile Red allowed us to distinguish between encapsulated oil and other droplet-like structures, which if examined by their shape alone could be mistaken as oil phase (**Figure 1**).

Using the confocal approach, we were able to optically dissect the particle in any desired number of coplanar cross sections to show the internal structure of fluorescently labeled gelatin as polymeric wall component. Such data can also be used to reconstruct the complete internal structure of the entire

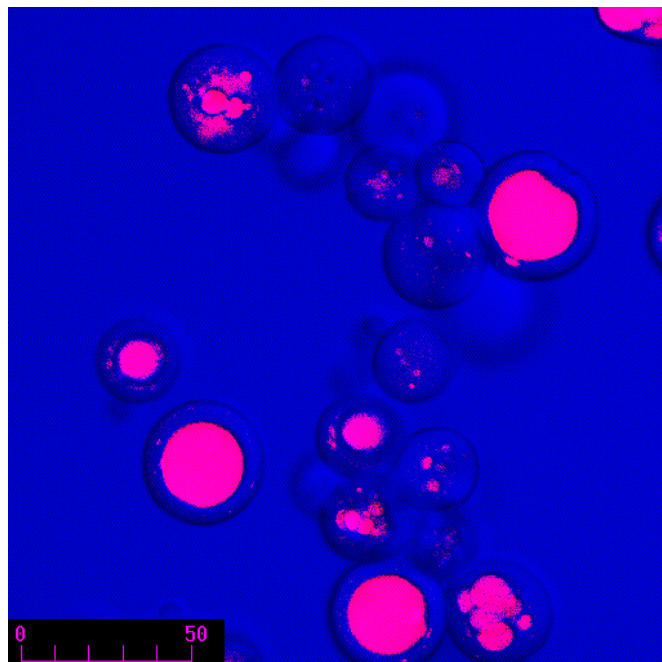


Figure 1. Microparticles Prepared by Complex Coacervation Containing EPA-EE as Oil Phase Fluorescently Stained with Nile Red.

*Scale bar is shown in μm .

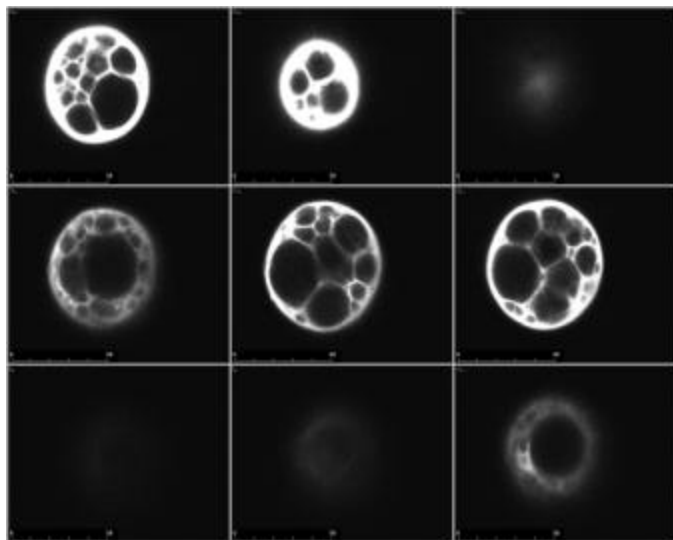


Figure 2. Three-dimensional Cross-Sectioning Through a Microparticle Prepared by Complex Coacervation After Covalent Labeling of Gelatin With RBITC.

microparticle (**Figure 2**).

The distribution of the polymers within the complex coacervation process was studied after fluorescence

labeling of each single polymer in separate batches. The polymer distribution was characterized by imaging fluorescence intensity across the depicted particle wall using computational image acquisition (**Figure 3**).

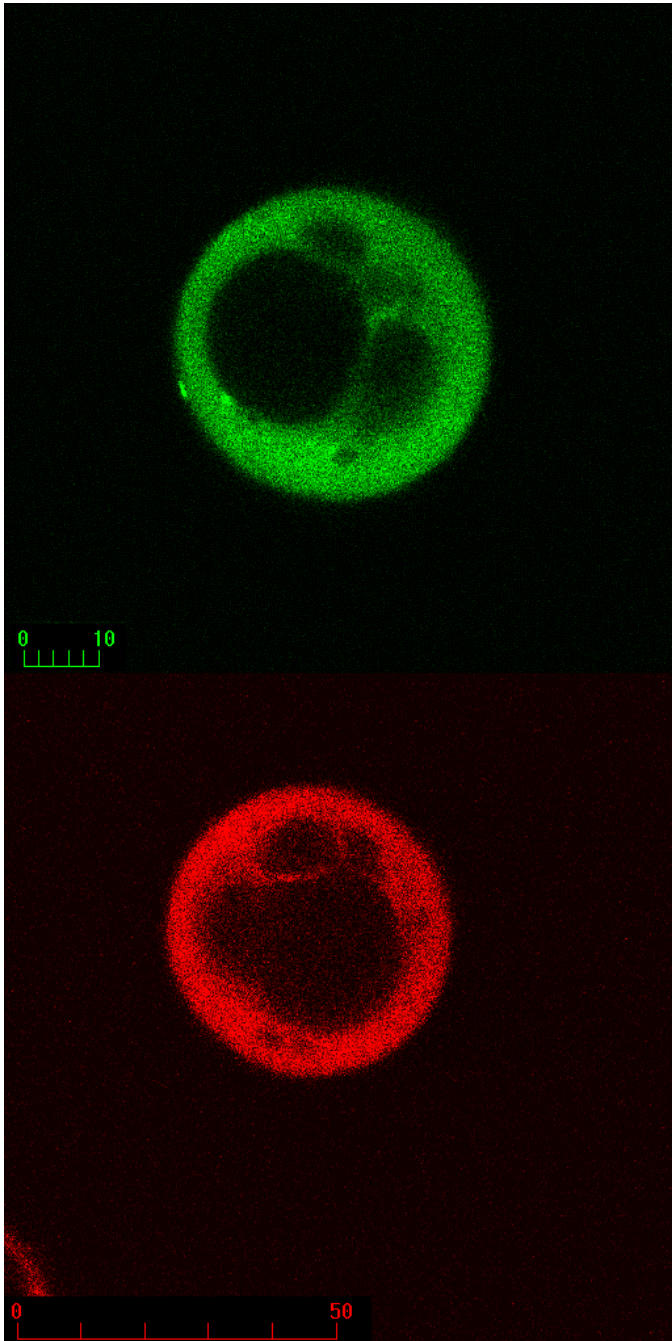


Figure 3. Sectioning of Microparticles Prepared by Complex Coacervation After Fluorescence Labeling of Gelatin With FITC (A) and Acacia With RBITC (B).

*Scale bar is shown in μm .

A homogeneous distribution for both gelatin and acacia was found throughout the particle wall. This was already found for the wall composition of microcapsules prepared by complex coacervation [12]. The internal structure of the microparticles in these experiments was formed by smaller aggregated oil droplets but showed, however, the same composition. Thus, this supports the hypothesis that phase separation takes place by electrostatic interaction of the oppositely charged polymers [16]. Due to the charge equivalence of the two polymeric counterions during coacervation, homogeneous distribution of both polymers inside the particle should be observed, which was supported by CLSM revealing a homogeneous distribution of the labeled polymers.

In order to visualize some heterogeneous distribution of different polymers within the particle wall, casein-FITC was added as a third component in the complex coacervation process. As shown in **Figure 4**, a maximum concentration of casein was found at the oil-wall interface (arrows), sharply decreasing toward the outer wall border.

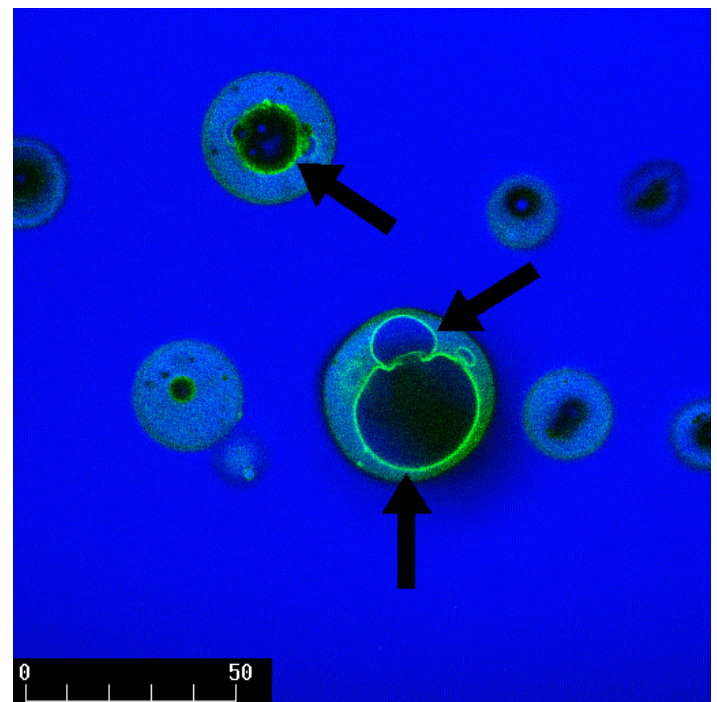


Figure 4. Image of Microparticles Prepared by Complex Coacervation with Non-Labeled Gelatin and Acacia Containing Additional Casein-FITC.

*Scale bar is shown in μm .

Concurrently, the distribution of gelatin and acacia indicated that their deposition was not influenced by the presence of casin-FITC (data not shown). For oil-in-water emulsions with mixtures of casein and gelatin, it is known that casein is the dominant component in lowering surface tension and therefore accumulates at the oil-wall interface [12, 17].

Deposition behavior during spray drying

The oil phase was emulsified in the gelatin solution, coacervated after adding acacia, and finally spray dried. Oil droplets in the emulsion were observed to be larger before hardening than the total microcapsule obtained after spray drying. Therefore, the emulsion was rearranged in its structure by the spraying process in such a way that the coacervate at the oil-water interface changed place during its passage through the sprayer nozzle. An explicit core/wall structure was observed to be independent from initial droplet size. CLSM imaging demonstrated that the homogeneous distribution of gelatin and acacia was retained throughout the capsule (**Figure 5**).

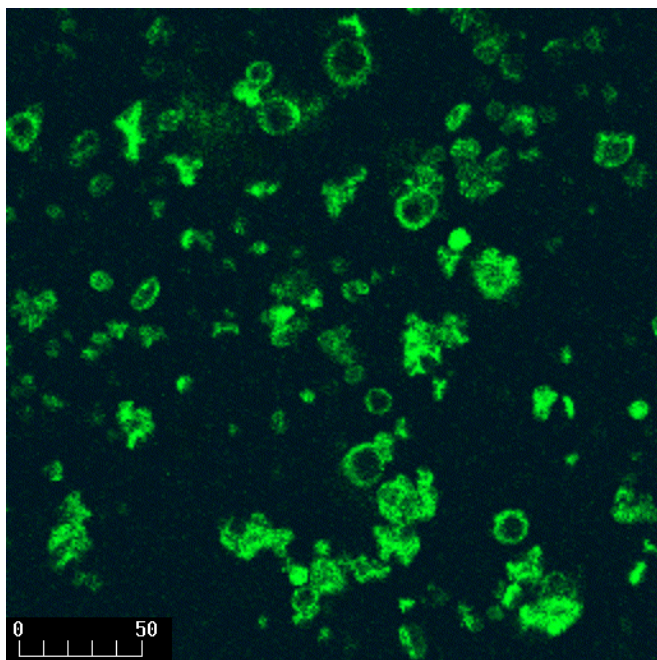


Figure 5. Image Representing the Microparticle Wall Composition with a View of Gelatin Labeled With FITC. Internal Structure of Microparticles After Spray Drying. *Scale bar is shown in μm .

As polymer properties are not likely to change during the spray-drying process, they keep both their interfacial activity and polyionic properties. This explains the observed homogeneous distribution in the coacervated particle wall. In addition to microcapsules, aggregates were also visible. These aggregates possessed concentrated polymer resulting in a more intense fluorescence signal. Therefore, heterogeneities marked by the fluorescence signal were present, but if one compares the capsule walls, homogeneous polymer distribution will be found.

The small size of the microparticles obtained after spray drying appeared to reach the limit of CLSM's resolution to depict their internal structure. In most cases, dry particles have to be used for the imaging, otherwise, fixation by resin embedding of the particle dispersion is required to avoid movement of the object during the imaging process. Particles smaller than $3\ \mu\text{m}$ in suspension tend to move and do not allow exact depiction. Besides, it appeared to us that it would be difficult to obtain a meaningful image resolution for microparticles smaller than $5\ \mu\text{m}$.

Deposition behavior during double emulsion technique

BSA was encapsulated as model protein drug into microspheres using the double emulsion technique. BSA is known to have surface active properties, which are responsible for its deposition at the oil-water interface [18]. This has a strong stabilizing effect on the first emulsion [19] and leads to the formation of a matrix-like structure (**Figure 6**).

The accumulation of BSA at the water-polymer interface might have been brought about the relatively low concentration of protein used in the preparation, so that most of the protein was found at the water-polymer interface.

The matrix structure of the microparticles prepared by the double emulsion technique is usually analyzed by SEM imaging of mechanical cross sections. Here, however, sectioning of particles occurs at random and cannot be controlled. In contrast, CLSM allows us to section the microcapsule at any desired plane (**Figure 7**).

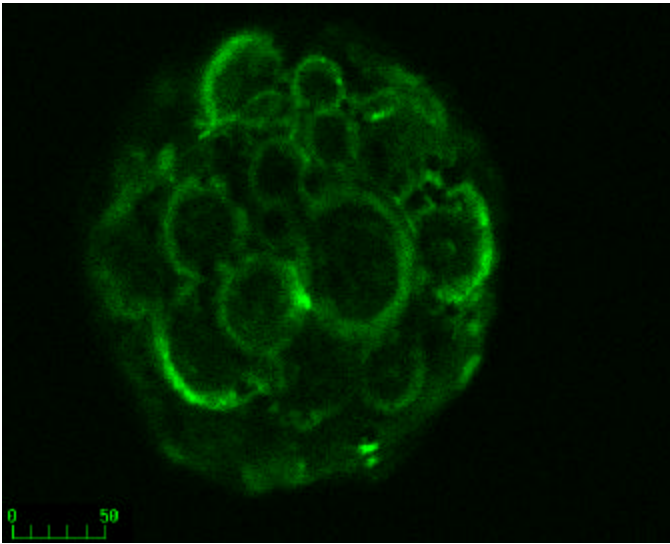


Figure 6. Microparticle Prepared by W/O/W Emulsification Solvent Evaporation Method Containing BSA-FITC as Model Protein Drug In the Internal Aqueous Phase. *Scale bar is shown in μm .

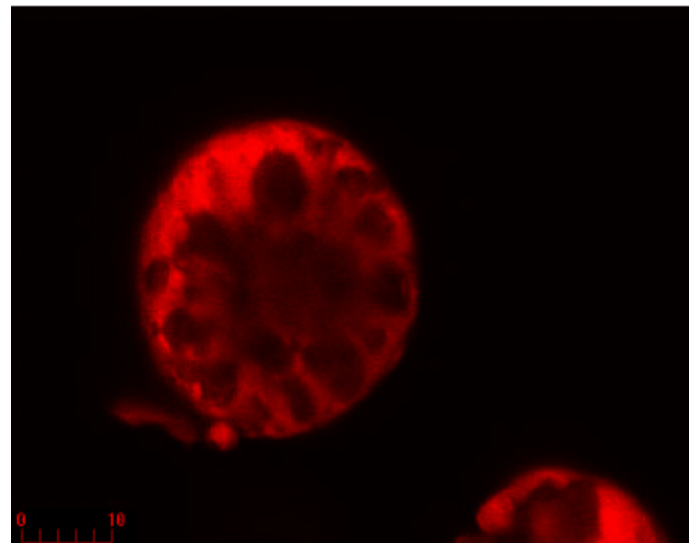
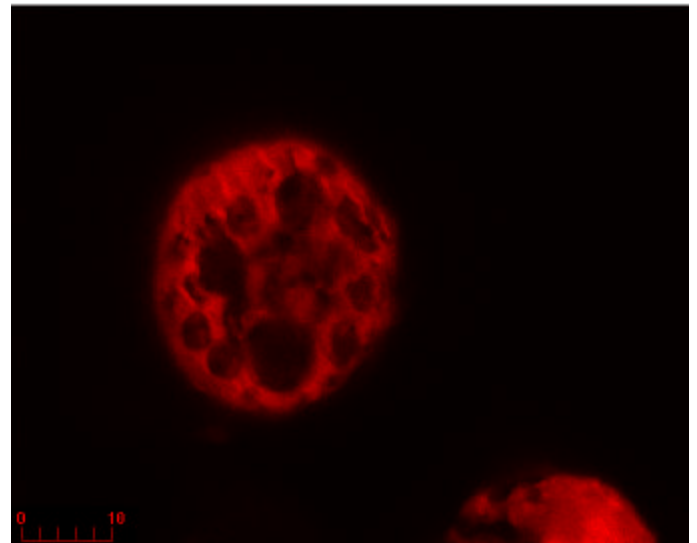
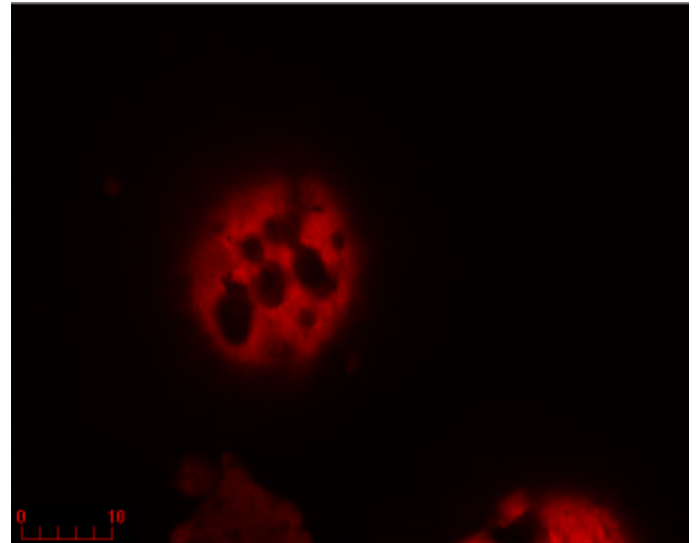


Figure 7. Coplanar Sections (Plane Distance: $5\ \mu\text{m}$) of the Internal Structure of a Microparticle Prepared by W/O/W Emulsification Solvent Evaporation Method Containing Nile Red in the Organic Phase. *Scale bar is shown in μm .

The limiting factor to image sectioning through the microparticle may be the transparency of the polyester. In deeper cross sections ($> 50\ \mu\text{m}$) the images still show the general structure, but they become blurred.

Deposition behavior during ionotropic gelation

The entrapment of compounds into alginate beads is another common technique that has been used in many applications. Here it may also be of interest to localize the incorporated drug. By using CLSM it was possible to localize the encapsulated FITC-BSA inside the alginate matrix (**Figure 8**).

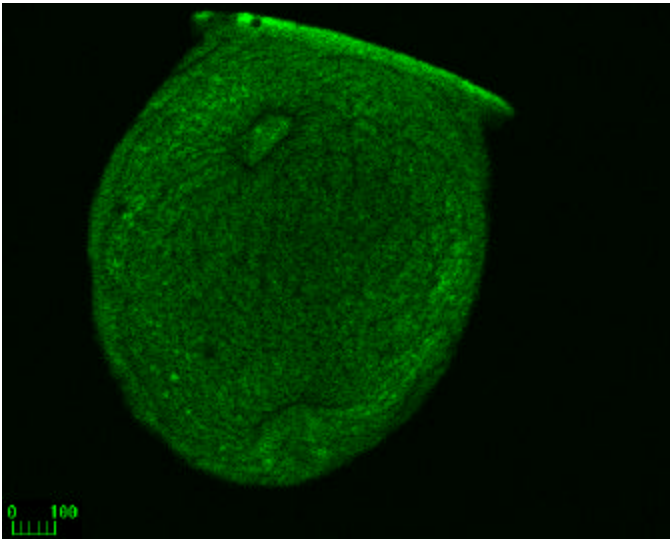


Figure 8. Image of Alginate Bead Prepared by Ionotropic Gelation Containing FITC-BSA as Fluorescently Labeled Model Protein Drug.

*Scale bar is shown in μm .

In general, a homogeneous distribution of the protein within the matrix was found. Moreover, we observed protein accumulation at the bead interface to the glass bottom of the drying device, while no heterogeneous deposition was found at the bead/air interface.

The preparation of alginate beads in presence of chitosan within calcium chloride solution has been reported elsewhere [20, 21]. By imaging with CLSM, the RBITC-labeled chitosan could be localized inside such beads and was proven to be distributed homogeneously throughout the bead matrix. The influence of chitosan presence on bead composition and protein localization was depicted by recording the signals of the two materials separately in different channels (**Figure 9**).

Until completely dry, the hydrogel matrix of alginate allows the movement of the protein, which may possibly interact with chitosan leading to some accumulation. Others have reported that incorporation of chitosan can lead to interactions with anionic compounds [22]. Sezer and Akbuga [20] incorporated dextran, which is not charged, and they therefore did not observe any interaction with chitosan inside the matrix. In our experiments, CLSM image procedure revealed that BSA was homogeneously distributed within the bead matrix, except for some accumulations

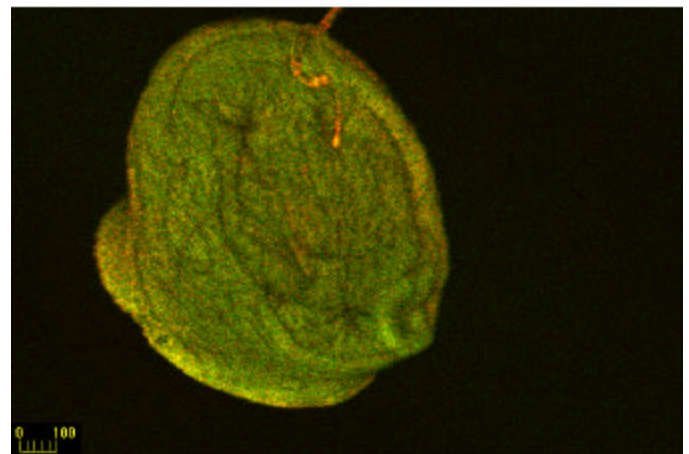
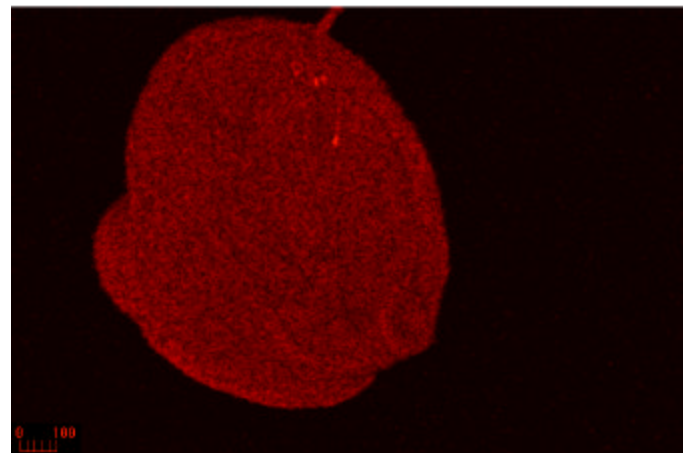
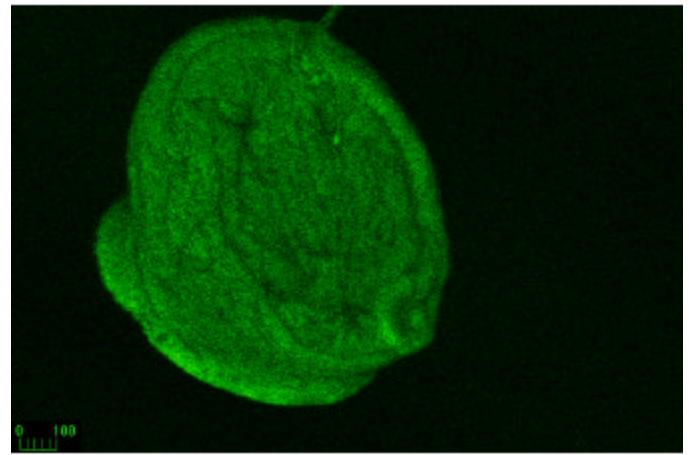


Figure 9. Images of Alginate Bead Prepared by Ionotropic Gelation in the Presence of Chitosan Including a Simultaneous Labeling of Protein and Chitosan, BSA-FITC Is Represented In Green, Chitosan-RBITC Is Represented In Red.

*Scale bar is shown in μm .

at the glass surface that occurred during the drying process. In the presence of chitosan, no increased concentration in the area of accumulated BSA was detected, therefore, it should be concluded that there is no strong interaction between protein and chitosan. Any subsequent differences in drug release profiles observed in the presence or absence of chitosan probably result from the different matrix properties of the beads rather than from potential interactions with the protein.

It must be noted, however, that an interference of the two fluorescence marker signals cannot be excluded. As the emitted signal from FITC may contribute to the excitation of RBITC, this double labeling system cannot be used for quantitative determinations of the fluorescently labeled polymers. Therefore, simultaneous visualization of the two FITC- and RBITC-labeled polymers must be proven by a single labeling of each polymer and separate visualization. Using another type of laser light, (eg, krypton/argon laser) and another set of noninterfering fluorescent probes should allow simultaneous quantitation of different polymers.

CONCLUSION

CLSM was shown to be a helpful tool for microparticle characterization. Using this relatively simple method, drug and polymer can be simultaneously visualized and unambiguously identified within the particles. This is hardly possible by other microscopic methods. Additional information on polymer composition and distribution throughout the particle wall can be obtained by CLSM. Furthermore, drugs and excipients can be localized three-dimensionally inside or on the surface of microparticles after fluorescence labeling. In general, CLSM appeared to us a very powerful technique for the characterization of microparticulate drug carriers, one that is easy to use and that provides more information than other microscopical inspection methods.

ACKNOWLEDGEMENTS

We would like to thank Sören Schwarzbeck and Dirk Neumann for their support with the computer image processing.

REFERENCES

1. Arneodo C, Benoit JP, Thies C. Etude préliminaire de la microencapsulation d'huiles essentielles par coacervation complexe. *STP Pharma Sciences*. 1986; 2:303-306.
2. Benoit JP, Thies C. Microencapsulation - methods and industrial applications. In: Benita S, ed. *Drugs and the Pharmaceutical Sciences*. , Vol. 73. New York: Marcel Dekker;1996.
3. Benita S, Benoit JP, Puisieux F, Thies C. Characterization of drug-loaded poly(*d,l*-lactide) microspheres. *J Pharm Sci*. 1984;73:1721-1724.
4. Mathews BR, Nixon JR. Surface characteristics of gelatin microcapsules by scanning electron microscopy. *J Pharm Pharmacol*. 1974;26:383-384.
5. Bodmeier R, McGinity J. Polylactic acid microspheres containing quinidine base and quinidine sulphate prepared by the solvent evaporation technique. I. Methods and morphology. *J Microencapsul*. 1987;4:279-288.
6. Cutts LS, Hibberd S, Adler J, Davies MC, Melia CD. Characterising drug release processes within controlled release dosage forms using the confocal laser-scanning microscope. *J Controlled Rel*. 1996;42:115-124.
7. De Smedt SC, Meyvis TKL, Van Oostveldt P, Demeester J. A new microphotolysis based approach for mapping the mobility of drugs in microscopic drug delivery devices. *Pharm Res*. 1999;16:1639-1642.
8. Bouillot P, Babak V, Dellacherie E. Novel bioresorbable and bioeliminable surfactants for microsphere preparation. *Pharm Res*. 1999;16:148-154.
9. Adler J, Jayan A, Melia CD. A method for quantifying differential expansion within

- hydrating hydrophilic matrixes by tracking embedded fluorescent microspheres. *J Pharm Sci.* 1999;88:371-377.
10. Rojas J, Pinto-Alphandary H, Leo E, Pecquet S, Couvreur P, Gulik A, Fattal E. A polysorbate-based non-ionic surfactant can modulate loading and release of beta-lactoglobulin entrapped in multiphase poly(DL-lactide-co-glycolide) microspheres. *Pharm Res.* 1999;16:255-260.
 11. Caponetti G, Hrkach JS, Kriwet B, Poh M, Lotan N, Colombo P, Langer R. Microparticles of novel branched copolymers of lactic acid and amino acids: preparation and characterization. *J Pharm. Sci* 1999;88:136-141.
 12. Lamprecht A, Schäfer UF, Lehr, CM. Characterisation of microcapsules by confocal laser scanning microscopy: analysis of structure, capsule wall composition and of encapsulation rate. *Eur J Pharm Biopharm.* 2000;49:1-9.
 13. Alex R, Bodmeier R. Encapsulation of water-soluble drugs by a modified solvent evaporation method. I. Effect of process and formulation variables on drug entrapment. *J Microencapsul.* 1989;7:347-355.
 14. Iwata M, McGinity JW. Preparation of multiphase microspheres of poly(lactic acid) and poly(lactic-co-glycolic acid) containing a W/O emulsion by a multiple solvent evaporation technique. *J Microencapsul.* 1992;9:201-214.
 15. Schreiber AB, Haimovich J. Quantitative fluorometric assay for detection and characterization of Fc receptors. *Meth Enzymol.* 1983;93:147-155.
 16. Luzzi LA, Gerraughty RJ. Effects of selected variables on the extractability of oils from coacervate capsules. *J Pharm Sci.* 1964;53:429-431.
 17. Mussellwhite PR. The surface properties of an oil-water emulsion stabilized by mixtures of casein and gelatin. *J Colloid and Interface Science.* 1966;21:99-102.
 18. Boury F, Ivanova T, Panaiotov I, Proust JE. Dilatational properties of adsorbed poly(D,L-lactide) and bovine serum albumin monolayers at the dichloromethane/water interface. *Langmuir.* 1995;11:1636-1644.
 19. Nihant N, Schugens C, Grandfils C, Jerome R, Teyssie P. Polylactide microparticles prepared by double emulsion/evaporation technique. I. Effect of primary emulsion stability. *Pharm Res.* 1994;11:1479-1484.
 20. Sezer AD, Akbuga J. Release characteristics of chitosan treated alginate beads: I. Sustained release of a macromolecular drug from chitosan treated alginate beads. *J Microencapsul.* 1999;16:195-203.
 21. Hari PR, Chandy T, Sharma CP. Chitosan/calcium alginate microcapsules for intestinal delivery of nitrofurantoin. *J Microencapsul.* 1996;13:319-329.
 22. Murata Y, Toniwa S, Miyamoto E, Kawashima S. Preparation of alginate gel beads containing chitosan nicotinic acid salt and the functions. *Eur J Pharm Biopharm.* 1999;48:49-52.